World Journal of Engineering and Technology, 2025, 13(3), 536-555
https://www.scirp.org/journal/wjet
ISSN Online: 2331-4249
ISSN Print: 2331-4222

Deformation Control and Early Warning Analysis of Deep Riverside Foundation Pit Construction Process Based on Machine Learning

Zunquan Zhu[1], Dongming Chang[1], Fang Xu[2], Mingtian Ma[2], Kai Zhang[2*]

[1]China Communications Third Shipping Engineering Bureau Co., Ltd., Shanghai, China
[2]School of Civil Engineering, Wuhan University, Wuhan, China
Email: *2020202100024@whu.edu.cn

How to cite this paper: Zhu, Z.Q., Chang, D.M., Xu, F., Ma, M.T. and Zhang, K. (2025) Deformation Control and Early Warning Analysis of Deep Riverside Foundation Pit Construction Process Based on Machine Learning. *World Journal of Engineering and Technology*, **13**, 536-555.
https://doi.org/10.4236/wjet.2025.133035

Received: June 16, 2025
Accepted: August 5, 2025
Published: August 8, 2025

Abstract

The large deep foundation pit projects usually face complex geological conditions, with high possibility of engineering disasters and difficult construction technology. Foundation pit stability monitoring and control is essential to ensure construction quality. The traditional method of foundation pit monitoring is difficult to achieve real-time disaster early warning, missing the best time for structural reinforcement and causing great potential safety hazards. Based on specific engineering cases, this study obtains and analyzes the actual response data of the foundation pit project through real-time monitoring, and uses different neural network models to predict the deformation of the soil around the foundation pit. The results show that when the LSTM model is predicted backward to 25 days, the RMSE value is 0.395, and the accuracy of the model is significantly higher than that of BP and GA-BP neural networks. The maximum relative error is less than 0.06 in the range of 2.5 - 6.0 m key monitoring depth, which meets the construction safety requirements. The model is used to predict the horizontal displacement of soil in the key monitoring interval of X1 monitoring point in the medium and long term. It is found that the maximum deformation value in this area is controlled within a very low range of 1.0 mm, which is far lower than the warning value stipulated in the relevant engineering specifications. In theory, the risk of large-scale deformation or failure of foundation pit engineering is excluded. Based on the above deformation prediction analysis, the prediction and evaluation of the effectiveness of supporting measures are realized, which can provide reference for the establishment and optimization of early warning mechanism of foundation pit deformation in similar projects. This study is of great significance for the early warning of foundation pit stability and the elimination of hidden dangers, which is helpful to further improve the quality and efficiency of engineering, reduce costs, and promote the scientific and standardized construction of foundation pit engineering.

Keywords

Deep Foundation Pit Engineering, Stability Monitoring, Horizontal Displacement, Machine Learning, Neural Network, Deformation Prediction

1. Introduction

As urbanization accelerates, high-rise buildings and the use of underground spaces encounter increasingly complex geological environments, more variable external factors, and greater technical challenges [1]. In large deep foundation pit projects under complex geological conditions, complex engineering problems such as stratum sliding and instability of support structures often occur. Therefore, on the basis of controlling project quality, developing effective foundation pit monitoring and early warning technologies is of significant importance for ensuring the safe construction and healthy operation of foundation pit projects [2].

Displacement monitoring of foundation pits primarily employs preset array displacement meters, strain gauges, and other deformation monitoring instruments to regularly or in real time detect horizontal and vertical displacements of foundation pit retaining structures, surrounding soils, or adjacent buildings during construction and use [3], and compare these with preset safety thresholds to predict or assess potential hazards in foundation pit structures in advance [4]. For areas that may pose safety risks, timely measures such as reinforcing support structures or adjusting construction plans are implemented to ensure the safety and stability of large deep foundation pit construction and use processes [5] [6]. Groundwater level monitoring is a crucial aspect of deep foundation pit projects, using water level gauges and other equipment to monitor changes in groundwater around the foundation pit, including parameters such as water level, pressure, and flow [7]. Timely understanding of the replenishment and discharge of groundwater around the foundation pit helps prevent geological disasters and construction risks caused by fluctuations in groundwater [8]. Additionally, groundwater level monitoring provides important hydrogeological data for foundation pit construction, guiding contractors to arrange construction plans reasonably and take appropriate protective measures. For instance, timely pumping or injection of water can prevent foundation pit flooding due to excessively high groundwater levels or geological collapse due to excessively low levels [9].

Traditional methods for foundation pit monitoring struggle to achieve real-time disaster early warning, often missing the optimal timing for structural reinforcement and posing significant safety risks [10]. Computer-aided intelligent analysis can scientifically predict time-varying nonlinear deformations of foundation pits [11]. The BP neural network was first proposed by foreign scholars at the end of the 19th century; it is a multilayer feedforward neural network trained according to the error backpropagation algorithm and is one of the most widely used neural network models currently. In recent years, the BP neural network model has been widely applied in foundation pit monitoring. Zhao Zhen [12], based on monitoring data from a foundation pit monitoring point in Taiyuan, established a BP neural network model to verify subsequent data, proving that the predictive accuracy of the BP neural network model meets the requirements for engineering applications. Li Wei *et al.* [13] established an improved BP neural network prediction model based on particle swarm optimization algorithms for monitoring foundation pit deformations, which proved the model's reliability through construction trials and provided effective support for safe construction. Zhang Deyu [14] proposed a foundation pit deformation monitoring method based on the BP neural network, demonstrating the economic benefits of neural networks in foundation pit monitoring through engineering examples. Meng Guowang *et al.* [15] proposed a method combining machine learning for multi-step rolling prediction of horizontal displacements of retaining structures, confirming that the prediction errors under three working conditions met the requirements through comparison with predicted results. Research by these scholars indicates that the machine learning method is a technology that can meet the requirements of foundation pit prediction and early warning in terms of accuracy and timeliness, widely used in engineering construction with good applicability.

This paper combines the large deep foundation pit project of the Unigroup New Intelligent Base in Xiaoshan District, Hangzhou, using relevant instruments for real-time monitoring to obtain actual response data of the foundation pit project. It employs the BP neural network model to conduct displacement prediction and early warning analysis of deep soil near the foundation pit retaining structure, promptly identifying and eliminating potential safety risks and unstable factors in the project to ensure the security and stability of the foundation pit project. This research contributes to further improving engineering quality and efficiency, reducing costs, and promoting scientific and standardized management in construction projects.

2. Project Introduction

2.1. Project Example Introduction

The Unigroup New Intelligent Base project in Xiaoshan District, Hangzhou, covers a total planned land area of 45,549.00 m^2, with a total construction area of 140,191.29 m^2. The main structures planned include two 11-story R&D buildings, two 13-story dormitory buildings, one 5-story factory building, one 2-story ancillary service building, one 2-floor staff activity center, and podium buildings and other ancillary facilities. There is one basement level beneath the site. The surrounding environment of the foundation pit is shown in **Figure 1**.

Figure 1. Surrounding environment of foundation pit.

The foundation type adopted for the project is bored pile foundation. The excavation area of the foundation pit is 30,530 m^2, with a perimeter of 730 m. The excavation process of the foundation pit utilizes a combination of lattice struts and PC (prefabricated concrete) method pile composite support construction. The retaining piles consist of Φ630 × 14 PC method composite steel pipe piles plus Larsen IV steel sheet piles.

2.2. Stratum Lithologic

According to the drilling exposure, within the exploration depth range of this site, the strata can be divided into six major engineering geological layers based on their types and differences in physical and mechanical properties, further subdivided into 11 sublayers. The spatial distribution of each rock and soil layer is shown in Figure 2.

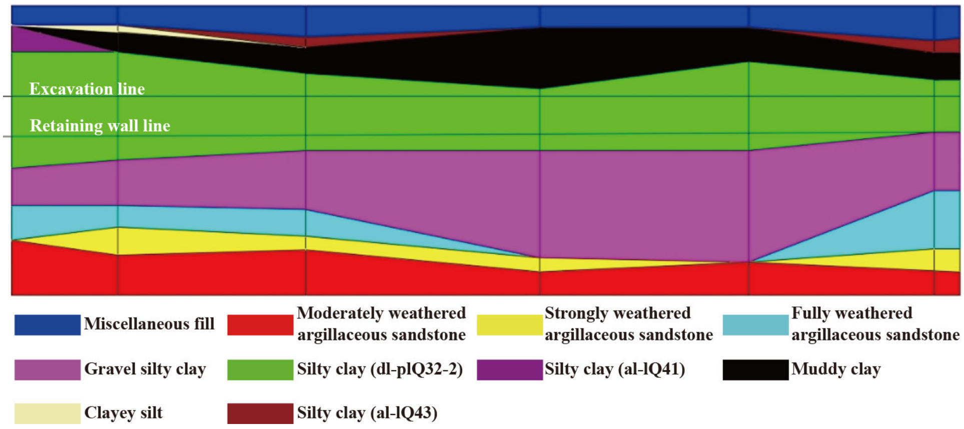

Figure 2. Engineering geology profile.

The physical and mechanical property parameters of each rock and soil layer are described from top to bottom as shown in Table 1:

Table 1. Physical and mechanical property index of soil layer.

Soil layer number	Soil layer name	Gravity γ (kN/m³)	Vertical permeability coefficient K_h (cm/s)	Vertical permeability coefficient K_v (cm/s)	Internal friction angle φ (˚)	Cohesive force c (kPa)
I	Miscellaneous fill	/	/	/	/	/
II	Silty clay 1	18.9	5.00×10^{-6}	4.27×10^{-6}	9.6	16.0
III	Clayey silt	19.2	8.26×10^{-5}	7.88×10^{-6}	21.5	8.4
IV	Muddy clay	17.4	4.40×10^{-6}	3.80×10^{-6}	1.6	5.6
V	Silty clay 2	18.8	1.12×10^{-6}	1.00×10^{-6}	8.0	14.4
VI	Silty clay 3	19.7	6.90×10^{-6}	5.79×10^{-6}	10.6	36.8

2.3. Geohydrologic Condition

Based on the investigation and exploration in the survey report, a newly opened river is distributed to the west outside this site, with a width of approximately 20 meters. During the survey period, the water depth of the river was measured to be about 1.5 to 2.0 meters, and the elevation of the river surface was around 3.0 meters. There is a close hydraulic connection between the river and the groundwater at this site, directly influencing the recharge and discharge relationships.

The pore water table at this site is primarily contained within the layers of soil, including the I layer of miscellaneous fill, the II layer of silty clay, the III layer of clayey silt, and the IV layer of mucky clay. The stable groundwater level was measured during the survey period to have a depth ranging from 0.30 to 4.20 meters. The annual fluctuation range of the groundwater level is approximately 1.0 to 2.0 meters, and the highest groundwater level in recent 3 to 5 years has approached the surface level.

2.4. Poor Geological Conditions

Within the project site, there are extensive fishponds present, which after being backfilled and leveled, have formed hidden ponds. These pose challenges for pile foundation construction and excavation work, particularly located within the pit area as well as to the west and northeast sides. The backfill has been completed, but the soil structure is loose, its composition is mixed, and its properties vary significantly, indicating it is recently backfilled soil.

To the south of the site, there is a layer of silty clay with a thickness of 3.5 to 5.5 meters, distributed 3.3 to 5.2 meters below ground level. In the central western part of the site, localized areas contain silty clay with a thickness of 9 to 11 meters, found 4 to 5 meters beneath the surface. To the north of the eastern side, there is a thicker layer of miscellaneous fill, approximately 7 meters deep, with a local presence of about 14 meters of silty clay beneath it. On the southern side of the east, the miscellaneous fill is thinner, with silty clay buried at a depth of approximately 1.2 to 5.2 meters thick, with a total thickness of about 5 to 6 meters. To the north of the site, the shallow layer of miscellaneous fill is relatively thick, about 7 meters, underlain by better-quality silty clay with no distribution of silty soil.

2.5. Layout of Monitoring Points for Foundation Pit Stability

Monitoring points prioritized horizontal displacement and groundwater levels as critical stability indicators, selected based on historical failure mechanisms in riverside mega-excavations and real-time safety protocols. These dominant risk factors were continuously tracked at key locations to capture their interdependent behavior through machine learning-driven analysis.

1) Observation of Horizontal Displacement of Deep Soil Masses

Along the periphery of the excavation pit, deep soil displacement inclinometer casings are installed according to the diagram provided. The casing holes for the basement area extend 3 meters deeper than the retaining piles. Lateral displacement is highly sensitive during excavation and serves as a critical indicator to determine the safety of the support system [16]. The horizontal displacement of deep soil masses around the pit is observed and collected using the Huashi Control ADM series array inclinometer casings. As shown in **Figure 3**, the monitoring points for soil horizontal displacement are numbered X1 through X20.

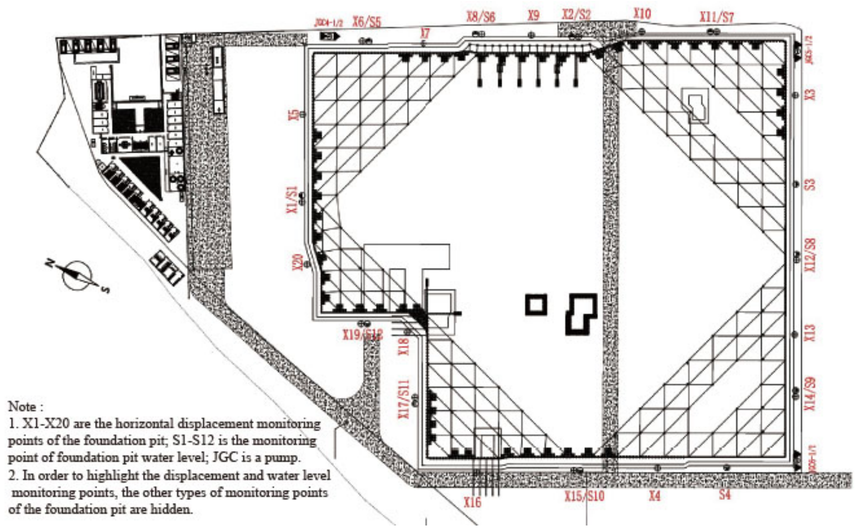

Figure 3. Layout of pit monitoring points.

2) Groundwater Level Monitoring

Groundwater observation pipe holes are buried on the inner and outer sides of the pit's surface according to the diagram provided, to monitor changes in the water table outside the pit during excavation and operation. By combining observations from these wells, the monitoring points for the external phreatic water level should be spaced along the longitudinal axis of the pit at intervals of 20 to 50 meters, with at least one point at each end of the pit. In areas with complex hydrogeological conditions, the density of monitoring points should be increased appropriately. These points should preferably be arranged at locations such as the connections of diaphragm walls, the overlaps of mixing pile construction, corners, near adjacent buildings (structures), areas with dense underground pipelines, and they should ideally be placed about 2 meters outside the waterproof curtain. As depicted in **Figure 3**, the groundwater level monitoring points are numbered S1 through S12.

3. BP Neural Network Foundation Pit Monitoring Modeling

3.1. BP Neural Network

Back Propagation (BP) neural network is a multilayer feedforward machine learning method based on the gradient descent algorithm, also known as the error backpropagation multilayer feedforward neural network. It is a multi-layer feedforward network trained by the error backpropagation algorithm. Its principle involves training and learning input samples to analyze the mapping relationship between sample parameters, making it highly suitable for solving nonlinear problems [17]. It is one of the most widely used neural network models and also one of the most theoretically mature neural network [18]. The BP neural network typically includes an input layer and an output layer, as well as one or more hidden layers. This special structure solves the problem of difficulty in learning for hidden layers, which was a constraint on the development of multilayer neural networks, allowing multilayer networks to effectively address highly nonlinear mapping issues. The learning process of the BP neural network consists of two processes: forward propagation and backward propagation. **Figure 4** illustrates the forward propagation of the BP neural network. The learning samples x_1 - x_n serve as input information, entering from the input layer. After being processed by the weights and thresholds of the hidden layer, they are transmitted to the output layer, ultimately resulting in output values y_1 - y_m. It is important to note that when the output value has a large error, the error backpropagation continues. The weights connecting the layers are adjusted based on the error information to reduce the error, eventually achieving the desired output [19].

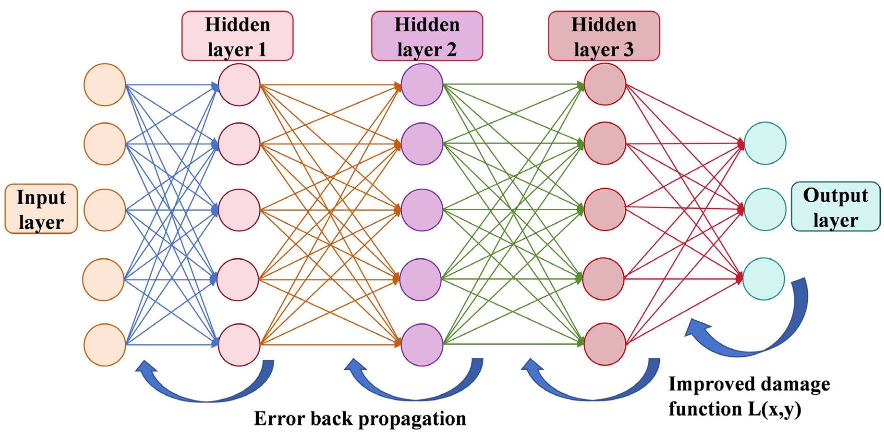

Figure 4. Topological structure of neural network.

The BP neural network is used to train and predict the horizontal displacement of the soil around the foundation pit. The establishment and training process of the model mainly includes the following steps:

1) Determination of Input and Output Layers

As the construction environment of the foundation pit evolves over time, predicting data for the next construction phase through measured data can effectively avoid interference from other factors and minimize the impact of human factors. The 71st displacement value was predicted by 70 consecutive deformation data, so there were 70 neurons in the input layer and 1 neuron in the output layer.

2) Determination of Hidden Layer Node Numbers

First, three methods are employed to obtain the number of hidden layers, leading to three different counts. We identify the minimum and maximum node numbers and then verify the model prediction errors one by one starting from the minimum until reaching the maximum. Finally, we select the hidden layer node count with the smallest model error. The three methods are as follows:

$$n_1 = \sqrt{nm} \tag{1}$$

$$n_1 = \log_2 a \tag{2}$$

$$n_1 = a + \sqrt{n+m} \tag{3}$$

The final determination of the optimal range for the number of hidden layer nodes is [6] [17]. At this time, the model converges quickly, operates with small errors, and achieves high prediction accuracy. After experimental verification, it was found that when the number of hidden layer nodes is 10, the model error is minimal, and the effect is the best.

3) Selection of Training Samples

In this study, we utilize real measured deformation data of the foundation pit as the input quantity for the model. We select a total of 70 days of actual measured data from the beginning of the construction to the end of the foundation pit excavation as the training samples input into the model. These training samples cover the entire period of foundation pit excavation construction, enabling comprehensive and effective training of the model to achieve the purpose of engineering application.

3.2. GA-BP Neural Network

Genetic algorithm (GA) is a computational method that simulates natural selection and genetic mechanism, which is often used to solve optimization problems [20]. Through genetic algorithm optimization, BP neural network can obtain a better combination of weights and bias values, thereby improving prediction accuracy and generalization ability, and improving prediction efficiency [21].

The training scheme of GA-BP model includes: importing data files, and the time point prediction interval is 1. Read the main spatial variables, including training data, network parameters and optimization parameters. Decode the genetic algorithm chromosome, convert it into the weight and bias of the neural network, and write it into the network structure. After that, the samples are reshaped and segmented to form model input and output. In this process, the data is normalized and the data format is converted. A BP neural network with five hidden nodes is created as the initial training model. The genetic algorithm is used to optimize the weight and bias of the BP neural network, and the population parameters, accuracy, selection operator, etc. are set, trained and optimized. Then, the population initialization is carried out, and the genetic algorithm is optimized to calculate the optimal parameters of the population. Finally, according to the optimal parameters, the weight and bias information of the neural network are updated. The hyperparameters of the neural network are set as follows: the number of iterations is 1000, the target error threshold is 2×10^{-4}, and the learning rate is 0.01. The population initialization assignment is performed, the genetic algebra is 10, and the population size is 5.

3.3. LSTM Neural Network

Long short-term memory (LSTM) network is a special variant of recurrent neural network. The LSTM unit is composed of forgetting gate, input gate and output gate. It can determine whether the data is updated or discarded by the logic control of the gate unit, which overcomes the shortcomings of RNN weight influence, gradient disappearance and explosion, so that the network can converge better and faster, and can effectively improve the prediction accuracy [22].

In order to use LSTM neural network for time series prediction, the following key contents need to be processed. Firstly, the read data is cleaned and sorted into training set according to certain rules. After that, the structure of the neural network is defined, including input layer, LSTM layer, fully connected layer and regression layer, and the initial learning rate is set to 0.01. Then, adam solver is used to train the LSTM network for 1000 rounds. At the same time, the learning rate attenuation strategy is configured to monitor the training progress and display the training curve. Finally, the training data is standardized, and the previous data is used to predict the next step, and the backward cycle prediction is performed.

4. Monitoring and Analysis of Foundation Pit Stability

4.1. Horizontal Displacement of Deep Soil

In **Figure 3**, among a series of monitoring points for soil displacement in the foundation pit, monitoring points X1 and X4 are located in the middle of the surrounding retaining area of the pit near the river, monitoring point X2 is near the support point of the crown beam on the side away from the river, and monitoring point X3 is close to the corner point of the pit on the side away from the river. These four monitoring points have certain representativeness. Therefore, the horizontal displacements near these monitoring points are analyzed accordingly. The curve of soil horizontal displacement at different depths of inclinometer tubes X1 - X4 over time is shown in **Figure 5**.

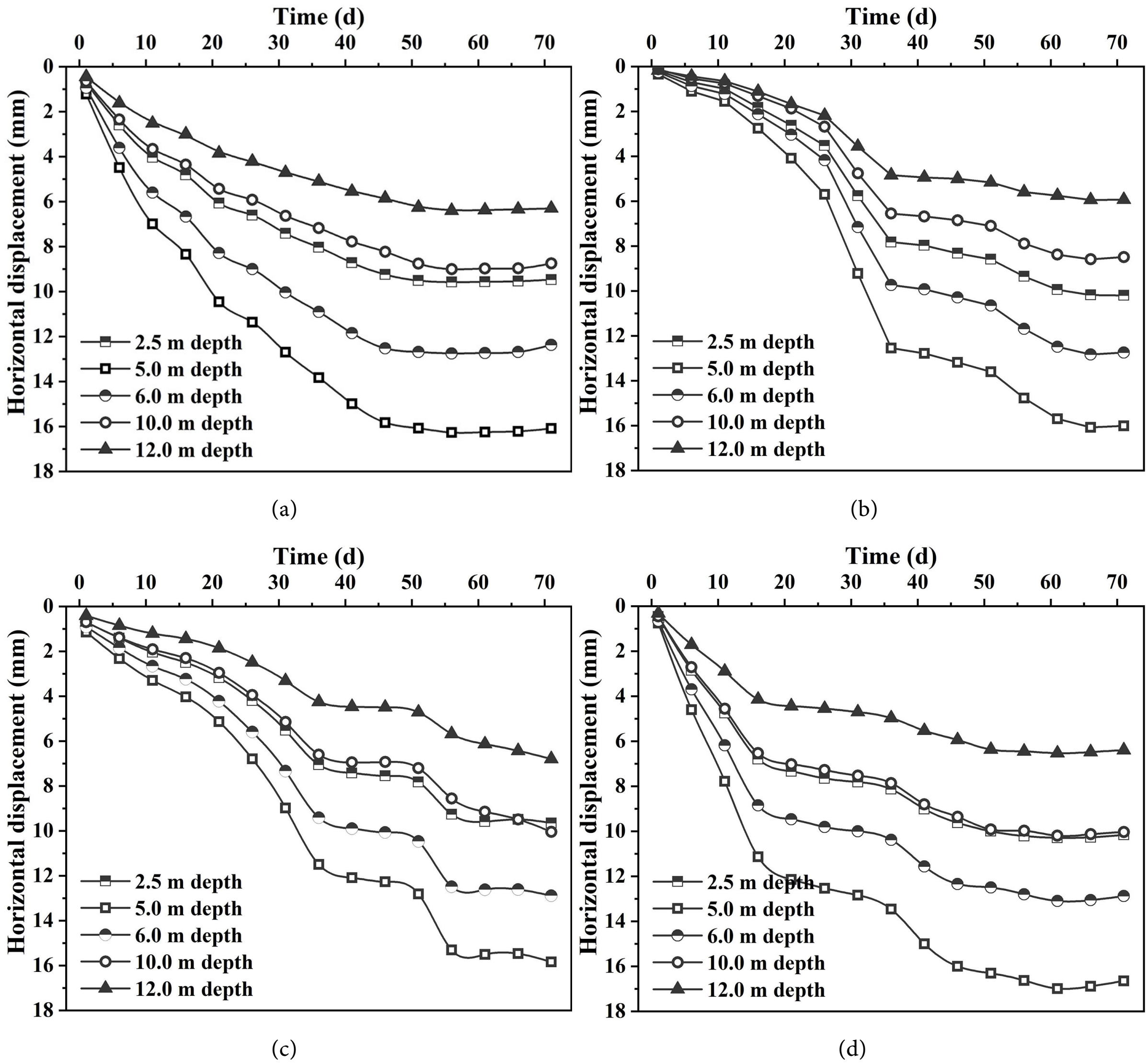

Figure 5. Change curve of soil horizontal displacement with time near the foundation pit retaining structure. (a) Horizontal displacement of soil at different depths of inclinometer X1; (b) Horizontal displacement of soil at different depths of inclinometer X2; (c) Horizontal displacement of soil at different depths of inclinometer X3; (d) Horizontal displacement of soil at different depths of inclinometer X4.

It can be observed that the trend of soil displacement changes at different monitoring points is similar. During the first 50 days of monitoring, the foundation pit is undergoing excavation. As the depth of excavation continuously increases, the surrounding soil pressure is redistributed under the influence of self-weight soil pressure and additional pressures from upper construction machinery, pedestrians, and surrounding buildings, causing a certain degree of horizontal displacement in the soil around the foundation pit [23]. This stage also sees the largest soil displacement. The monitoring points X1 - X4 show that the displacement values at different locations may differ due to spatial effects, being influenced differently by factors such as rock and soil layer distribution, groundwater level, and upper loads, but their maximum horizontal displacements all occur during this stage.

Starting from the 45th day, the foundation pit excavation ends and the cushion and foundation construction is completed. Meanwhile, the support system is fully constructed, significantly reducing the rate of foundation pit deformation and effectively suppressing the tendency of surrounding soil to shift towards the pit. From the 55th day onwards, the horizontal displacement at the monitoring points tends to stabilize.

Looking at the soil displacement at different depths, due to the combined use of lattice struts and PC pile joint support, the shallow soil deformation at about 2.5 m depth is relatively small, with the maximum horizontal displacement occurring at around 6.0 m depth, and the deep inclinometer curve showing a bulging shape in the middle. At depths greater than 12.0 m, the amount of soil horizontal displacement is very small, and in the stable stage after support, the maximum displacement is less than 6.0 mm.

Additionally, in **Figure 5**, it is observed that during the same period at the same depth, the horizontal displacement at monitoring points X1 and X4 is larger than that at X2 and X3. Analyzing this difference structurally, monitoring points X1 and X4 are located in the middle of the periphery of the foundation pit, where the soil pressure on the retaining structure is higher, and the stiffness of the struts and PC piles is limited, resulting in relatively larger horizontal displacements [24]. In contrast, monitoring point X3 is located near the corner point of the foundation pit, where the active soil pressure on the retaining structure can be relieved through arching effects, and the nearby soil deformation is usually the smallest in the foundation pit [25]. Monitoring point X2 is near the crown beam support, which has a large stiffness and can effectively restrict the deformation of the nearby retaining structure, so its horizontal displacement is also relatively small [26].

4.2. Change of Groundwater Level Around Foundation Pit

In the groundwater monitoring points shown in **Figure 3**, monitoring point S1 is adjacent to displacement monitoring point X1, and S4 is located near displacement monitoring point X4 outside the perimeter retaining area close to the river. Monitoring point S2 is adjacent to displacement monitoring point X2, while monitoring point S3 is located near displacement monitoring point X3 outside the perimeter retaining area far from the river. The changes in groundwater levels have a significant impact on the deformation and stability of the foundation pit. Therefore, by taking the water level variations at the four groundwater monitoring points S1 to S4 and combining them with the soil displacement data in section 4.2, an analysis of the foundation pit's stability can be conducted. The depth of groundwater levels at monitoring points S1 to S4 over time is depicted in **Figure 6**.

It can be observed that for monitoring points S1 and S4, which are closer to the river, during the first 50 days of monitoring, the water level outside the pit declined almost linearly, and after 55 days, the rate of decline significantly decreased.

Unlike S1 and S4, the monitoring points S2 and S3, which are farther from the river, experienced a noticeable lag effect in water level decline during excavation. For the first 15 days of monitoring, due to the longer drainage path, there was little change in the groundwater level, with some slight recovery and fluctuations. After 40 days of monitoring, the water level began to drop significantly and uniformly, with a higher rate of decline compared to the same period for monitoring points S1 and S4.

Analyzing the horizontal displacement of soil at X1 to X4 in conjunction with the changes in groundwater levels reveals that the maximum rate of horizontal displacement change occurred at points X1 and X4 within the first 15 days, while at points X2 and X3, the maximum rate of change occurred between 30 and 40 days. This lag is attributed to the delayed decline in water level at points X2 and X3, resulting in a delayed dissipation of pore water pressure, and consequently, a delayed consolidation and deformation of the soil. This difference also indicates that the change in groundwater level has a substantial influence on the development of horizontal displacement of soil around the foundation pit.

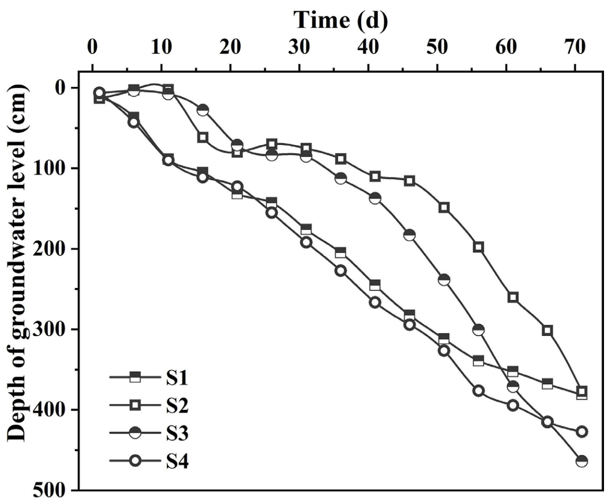

Figure 6. Change curve of groundwater level with time near foundation pit envelope.

During the first 50 days of monitoring, the groundwater level outside the pit exhibited a nearly linear decline. However, after 55 days, the rate of decline significantly decreased. In contrast to S1 and S4, the monitoring points S2 and S3, which are located away from the river, showed a distinct lag effect in the water level drop during excavation. For the initial 15 days of monitoring, due to the longer drainage path, the change in groundwater level was minimal, with slight recoveries and fluctuations observed. It was only after 40 days of monitoring that a significant and uniform decline in water level occurred, with a greater rate of decline compared to the same period for monitoring points S1 and S4.

Analyzing the horizontal displacement of soil at X1 to X4 in conjunction with the changes in groundwater levels revealed that the maximum rate of horizontal displacement change occurred at points X1 and X4 within the first 15 days, while at points X2 and X3, the maximum rate of change occurred between 30 and 40 days. This lag is attributed to the delayed decline in water level at points X2 and X3, resulting in a delayed dissipation of pore water pressure, and consequently, a delayed consolidation and deformation of the soil [27]. This difference also indicates that the change in groundwater level has a substantial influence on the development of horizontal displacement of soil around the foundation pit [28].

In the displacement monitoring, it was also observed that at the same time and depth, the horizontal displacement at monitoring points X1 and X4 was greater than at X2 and X3. Analyzing this discrepancy in terms of groundwater level changes, it is evident that because monitoring points X2 and X3 are farther from the river and have a relatively longer drainage path, the contemporaneous groundwater level in the vicinity of these measuring points was higher than that at X1 and X4. This resulted in a reduced tendency for soil to extrude into the pit due to the dissipation of pore water pressure.

5. Rationality Verification of Neural Network Model and Prediction Analysis of Foundation Pit Deformation

5.1. Model Training Effect

Combined with the above analysis, among several foundation pit monitoring points, the horizontal displacement of soil at X1 monitoring point is always relatively large, and the groundwater level is relatively high, which is the key position for foundation pit stability monitoring.

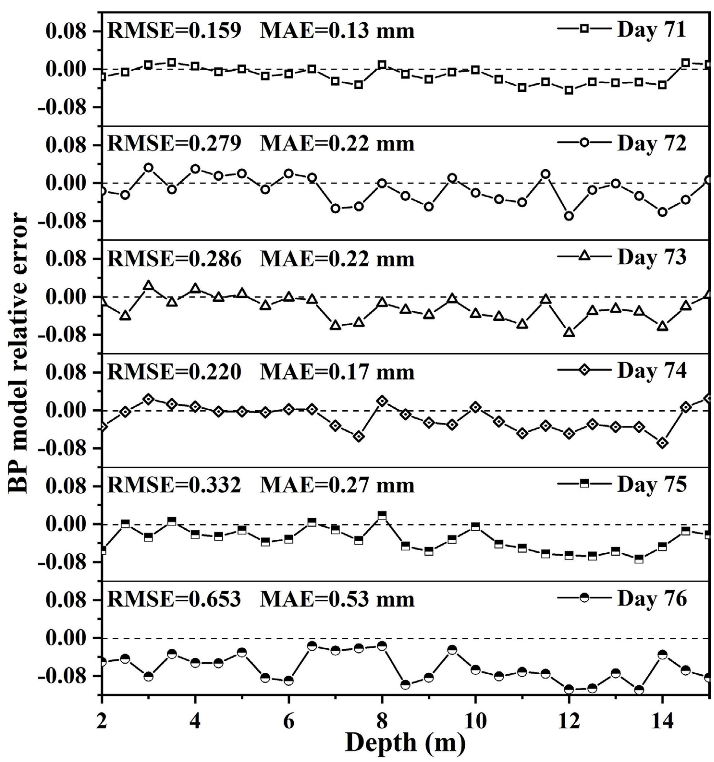

Figure 7. Relative error distribution based on BP neural network prediction.

A total of 70 records of soil horizontal displacement data at monitoring point X1, spanning the full 70-day evolutionary period (Days 0 - 70), were dedicated as the training set for neural network development. This duration comprehensively captures the critical deformation progression established in Section 4.1: an initial rapid deformation phase followed by progressive deceleration culminating in stabilized slow deformation. Crucially, post-Day 70 deformation extends this stabilized regime without introducing new failure mechanisms or acceleration trends. Upon completing model training, the finalized network was applied to forecast soil deformation at X1 for Days 71 - 100, generating depth-dependent horizontal displacement prediction curves. To dynamically validate model performance, these predictions were rigorously compared against actual monitoring values from the same period (Days 71 - 100). Prediction accuracy was quantified using mean absolute error (MAE) and root mean square error (RMSE) [29], with results visualized in **Figures 7-9**.

Figure 7 shows the relative error distribution of prediction results based on BP neural network. From the relative error value, most of the predicted values are less than the measured values. At the same time, it can also be observed from the diagram that the accuracy of the model gradually decreases with time. By the sixth day, the maximum relative error has exceeded 0.1, the RMSE is 0.653, and the MAE reaches 0.53 mm. This is because the deformation trend of foundation pit has time memory characteristics, that is, the past deformation history will have an impact on the future deformation trend. Due to the lag of training samples, the prediction model cannot accurately reflect this characteristic, thus affecting its prediction accuracy [30]. This also shows that there is still room for improvement in the prediction effect of the BP model, which still needs further optimization.

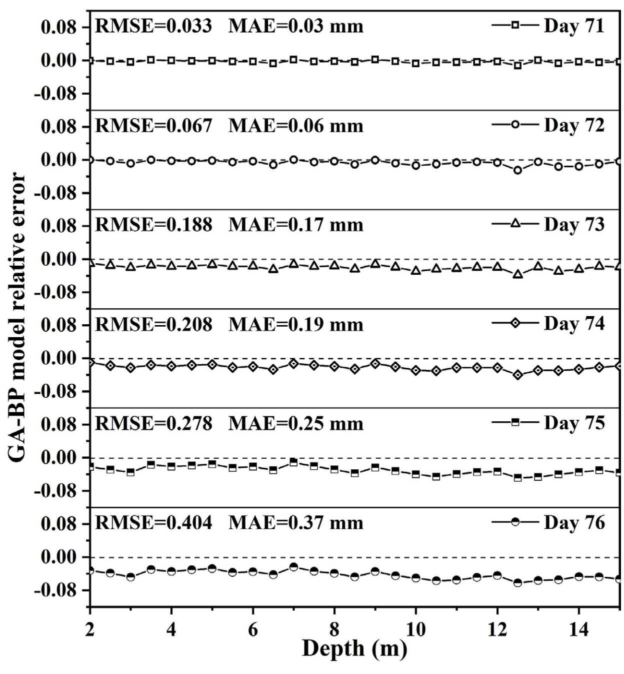

Figure 8. Relative error distribution based on GA-BP neural network prediction.

Figure 8 shows the relative error distribution of the prediction results based on GA-BP neural network. It can be seen from the diagram that the prediction effect of GA-BP neural network is obviously better than that of traditional BP neural network in the first 5 days. The maximum relative error is less than 0.04, the RMSE value is within 0.03, and the MAE is within 0.25 mm. It has high accuracy in short-term prediction. However, after the fifth day, the relative error of the predicted value gradually increased, and the prediction effect was close to the traditional BP neural network. At the same time, the GA-BP model also has the problem that most of the predicted values are less than the measured values with the extension of the prediction time. This may be due to the over-fitting of the BP model on the training set caused by genetic algorithm optimization, which makes it perform poorly in the test set or the actual data. The above results show that GA-BP neural network has a good backward short-term prediction effect (≤ 5 d) for this project, which is suitable as a prediction model for short-term deformation monitoring and control of foundation pit, but it does not perform well in backward long-term prediction.

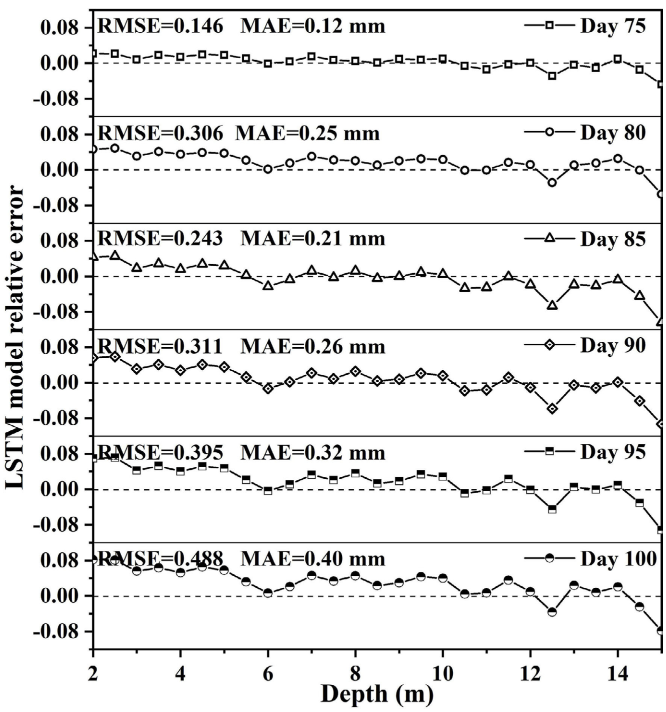

Figure 9. Relative error distribution based on LSTM neural network prediction.

Figure 9 shows the relative error distribution based on the prediction results of LSTM neural network, including the horizontal displacement of X1 monitoring point within 30 days from the 70th day. As can be seen from the diagram, the RMSE value of LSTM on the 5th day is 0.146, and the MAE is 0.12 mm. The above indicators are lower than the GA-BP model, indicating that it has higher accuracy in the depth range of the measuring point, and the effect of short-term predictive control is good. In the backward long-term predictive control, RMSE, MAE and the maximum relative error value have increased, and the model accuracy has a downward trend. This is because the influence caused by the excavation of the foundation pit cannot be calculated in the model. It needs to be solved by constantly updating the training samples and expanding the training set [31]. From the specific situation of the parameters, when the backward prediction time is 25 days, the RMSE value is 0.395, and the accuracy of the model is significantly higher than that of the GA-BP neural network. In the same period, the MAE value is 0.32 mm, and the maximum relative error in the key monitoring depth range of 2.5 - 6.0 m is less than 0.06, which meets the requirements of the construction scheme [32]. This shows that compared with the first two models, the LSTM neural network can still maintain high accuracy and relatively small error in a long-term backward prediction, which can provide a more effective reference for medium-long-term foundation pit deformation warning and engineering construction.

5.2. Foundation Pit Deformation Prediction

Following the validation of machine learning performance during the 71-100-day period, we executed medium-to-long term prospective forecasting to evaluate foundation pit stability. In order to study whether the soil deformation around the foundation pit will affect the stability of the foundation pit, we continue to pay attention to the key position X1 monitoring point of deformation monitoring, and carry out medium-long-term prediction of soil deformation near the maximum displacement deformation depth (4.0 - 6.0 m) of the soil. On this basis, the stability of the foundation pit project is analyzed. Combined with the analysis of the previous section, by updating the training samples, the LSTM model is used to predict the horizontal displacement of the soil at the X1 monitoring point in the depth range of 4.0 - 6.0 m. This updated model subsequently generated horizontal displacement predictions for Days 101 - 146, extending 46 days beyond the initial training horizon.

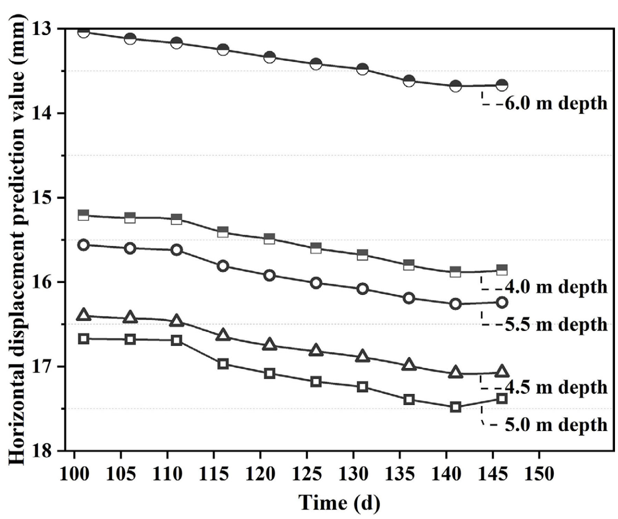

Figure 10. Medium-long-term prediction values of horizontal displacement of soil at different depths at X1.

The resulting forecasts (**Figure 10**) deliver critical insights into soil deformation evolution within this high-risk depth interval. It can be seen that during the 45 days prediction period, the maximum deformation at the X1 monitoring point is still near the depth of 5.0 m. During this period, for the key monitoring depth area of 4.0 - 6.0 m, the deformation of the soil is stable, and the maximum deformation is strictly controlled within the extremely low range of 1.0 mm, which is far lower than the warning value specified in the relevant engineering specifications [33]. From the perspective of deformation, it can be considered that the foundation pit structure has a certain ability to resist external unfavorable factors, and theoretically excludes the risk of large-scale deformation or damage. Based on the above deformation prediction analysis, it not only realizes the prediction and evaluation of the effectiveness of supporting measures, but also provides a reliable practical reference for the establishment and optimization of the early warning mechanism of foundation pit deformation in similar projects.

6. Conclusions

Deformation prediction and stability research are one of the key research directions in deep and large foundation pit engineering. Based on the deep and large riverside foundation pit project of Ziguang New Intelligent Base in Xiaoshan District of Hangzhou, this study obtains and analyzes the actual response data of the foundation pit project through real-time monitoring. Machine learning technology is used to predict the deformation of soil around the foundation pit, and the advantages and disadvantages of various neural network models are analyzed. Furthermore, combined with the appropriate model, the medium and long-term deformation of the deep soil near the retaining structure of the foundation pit is predicted, and the prediction and evaluation of the effectiveness of the support measures are realized. The main conclusions of this study are as follows:

1) The horizontal displacement of the soil outside the retaining structure of the foundation pit mainly occurs in the excavation stage, and there is a significant spatial effect. At the same depth in the same period, the horizontal displacement of the soil is the smallest near the negative corner of the foundation pit, the second near the support point of the crown beam, and the largest near the diagonal support around the foundation pit. By adopting the combined support of lattice bracing and PC pile in time, the deformation in the excavation stage can be effectively controlled.

2) In the foundation pit engineering near rivers and lakes, the speed of pore water pressure dissipation is different due to different drainage paths. The change of groundwater level away from the river is relatively lagging behind, which leads to significant differences in the change rate of horizontal displacement in each area of the foundation pit, and has a great influence on the maximum horizontal displacement value of the soil around the foundation pit. Therefore, in the process of foundation pit excavation, the drainage system should be reasonably arranged in different areas of the foundation pit according to the actual hydrogeological

conditions.

3) In this study, BP, GA-BP and LSTM models were used to train and predict the horizontal displacement values of key monitoring points. The comparison with the actual monitoring data shows that the maximum relative error is more than 0.1 and the RMSE is 0.653 when the BP model is used to predict the 6th day, and the accuracy is difficult to meet the requirements. The GA-BP model demonstrates high short-term forecasting accuracy, with maximum relative error <0.04 and RMSE <0.030 during the initial 5-day period. However, after the 5th day, the relative error of the predicted value increased significantly. When the LSTM model was predicted backward to 25 days, the RMSE value was 0.395, and the accuracy of the model was significantly higher than that of the GA-BP neural network. The maximum relative error is less than 0.06 in the range of 2.5 - 6.0 m key monitoring depth, which meets the construction safety requirements. It can provide a more effective reference for medium and long-term foundation pit deformation warning and engineering construction.

4) By updating the training samples, the LSTM model is used to predict the horizontal displacement of the soil at the X1 monitoring point in the depth range of 4.0 - 6.0 m. It is found that the maximum deformation value generated in this area is controlled within a very low range of 1.0 mm, which is far lower than the warning value stipulated in the relevant engineering specifications, and the risk of large-scale deformation or damage is excluded in theory. Based on deformation predictions, this analysis enables evaluating supporting measures and optimizing early-warning mechanisms for analogous projects. Future work will incorporate complementary parameters like stress responses to enhance predictive capabilities.

Conflicts of Interest

The authors declare no conflicts of interest regarding the publication of this paper.

References

[1] Zhou, Y., Zhu, Q.H., Zhu, Y.P., *et al.* (2019) Application Analysis of "One Dual-Purpose" New Support Structure in the Support of a Deep Foundation Pit. *Chinese Journal of Rock Mechanics and Engineering*, **39**, 3168-3177.

[2] Mo, P.Q., Liu, Y., Huang, Z.F., *et al.* (2012) Study on Deformation Coordination and Spatial Effect of Pile-Crown Beam-Support in Deep Foundation Pit under Complex Supporting Conditions. *Journal of Rock and Soil Mechanics*, **43**, 2592-2601.

[3] Xiong, Z.B. and Wang, Q.Y. (2009) Monitoring and Reinforcement of Horizontal Displacement of Support Structure for a Complex Plane Foundation Pit. *Rock and Soil Mechanics*, **30**, 572-576.

[4] Liu, X.Y., Chen, Z.J., Fu, S.F., *et al.* (2016) Finite Element Analysis of Monitoring and Deformation Influencing Factors of a Deep Foundation Pit. *Journal of Liaoning Technical University* (*Natural Science Edition*), **35**, 852-858.

[5] Ye, S.H. and Li, D.P. (2019) Monitoring and Numerical Simulation Analysis of Deep and Large Foundation Pit Excavation in Complex Environment. *Journal of Civil Engineering*, **52**, 117-126.

[6] Zou, Z.B. and Du, G.T. (2017) Analysis of Deep Foundation Pit Construction Monitoring Technology. *Highway Transportation Science and Technology* (*Applied Technology Edition*), **13**, 330-333.

[7] Yang, M., Zhu, Y.X., Zhao, D.B., *et al.* (2022) Research on Deep Foundation Pit Support and Groundwater Control Technology under Complex Conditions. *China Housing Facilities*, **10**, 64-66.

[8] Xu, X.F., Gong, Z.Y., Sun, Z.L., *et al.* (2022) Analysis of Deformation and Internal Force Monitoring Results of Ultra-Deep Circular Foundation Pit in Central Yunnan Water Diversion Project. *Journal of Civil Engineering*, **55**, 102-111. https://doi.org/10.1155/2022/7848152

[9] Xu, W., Xia, Q.W., Xu, P.F., *et al.* (2013) Monitoring and Analysis of Simultaneous Construction of Extra-Large Adjacent Deep Foundation Pit in Linjiang River on Soft Soil. *Chinese Journal of Rock Mechanics and Engineering*, **32**, 2676-2683.

[10] Wu, Z.J., Wang, H., Wang, S.L., *et al.* (2008) Development of Distributed Monitoring Information Management and Early Warning System for Foundation Pit. *Rock and Soil Mechanics*, **9**, 2503-2507+2514.

[11] Chen, H. (2020) Research on Deformation Prediction and Optimization of Foundation Pit. *Highway*, **65**, 414-418. (in Chinese)

[12] Zhao, Z. (2022) Application Research of Foundation Pit Deformation Prediction Based on BP Neural Network. *Shanxi Architecture*, **48**, 160-162.

[13] Li, W. and Deng, L.P. (2023) Monitoring and Analysis of Foundation Pit Deformation Based on BP Neural Network Model. *Surveying, Mapping and Spatial Geographic Information*, **46**, 140-143.

[14] Zhang, D.Y. (2023) Analysis and Application of Foundation Pit Deformation Monitoring Based on Neural Network. *Jiangxi Building Materials*, **7**, 163-164+167.

[15] Meng, G.X., Liu, J.L., Huang, J.S., *et al.* (2022) Research on Horizontal Displacement Prediction of Deep Foundation Pit Envelope Based on BP Artificial Neural Network. *Urban Rapid Transit*, **35**, 80-88.

[16] Li, H.T., Ren, G.M., Shen, G.Z., *et al.* (2023) Study on Deformation Control and Response of Deep Foundation Pit with Multiple Combination Supports under Complex Environment. *Journal of Chengdu University of Technology* (*Natural Science Edition*), **50**, 744-755.

[17] Qiao, Y. (2023) Research on Foundation Pit Deformation Prediction Based on BP Neural Network Model. *Building Technology*, **7**, 29-33.

[18] Zhao, Z. (2022) Application Research of Foundation Pit Deformation Prediction Based on BP Neural Network. *Shanxi Architecture*, **48**, 160-162.

[19] Liu, J., Li, F.H. and Liu, X.X. (2021) Optimization of GA-BP Neural Network Model and Prediction of Foundation Pit Deformation. *Tunnel Construction* (*Chinese and English*), **41**, 1733-1739.

[20] Wu, S., Zhao, G. and Wu, B. (2022) Real-Time Prediction of the Mechanical Behavior of Suction Caisson during Installation Process Using GA-BP Neural Network. *Engineering Applications of Artificial Intelligence*, **116**, Article 105475. https://doi.org/10.1016/j.engappai.2022.105475

[21] Zhang, W.S., Yuan, Y., Long, M., *et al.* (2024) Prediction of Surface Settlement around Subway Foundation Pits Based on Spatiotemporal Characteristics and Deep Learning Models. *Computers and Geotechnics*, **168**, Article 106149. https://doi.org/10.1016/j.compgeo.2024.106149

[22] Ye, X.W., Ma, S.Y., Liu, Z.X., *et al.* (2024) LSTM-Based Deformation Forecasting for

Additional Stress Estimation of Existing Tunnel Structure Induced by Adjacent Shield Tunneling. *Tunnelling and Underground Space Technology*, **146**, Article 105664. https://doi.org/10.1016/j.tust.2024.105664

[23] Tang, S., Jin, Q., Wang, W.L., *et al.* (2023) Research on Displacement Monitoring of Deep Foundation Pit of Large Structural Foundation in Low Altitude Area. *Industrial Building*, **53**, 411-415+428.

[24] Huang, L.W., Xu, C.L., Zhou, K., *et al.* (2024) Foundation Pit under Complicated Environment Condition in Soft Soil Area Collapse Cause Analysis. *Journal of Underground Space and Project*, **20**, 1039-1050.

[25] Feng, Q., Qin, C., Zheng, S.L., *et al.* (2016) Effect Analysis of Positive Angle and Negative Angle of Foundation Pit. *Sichuan Cement*, **12**, 292-293.

[26] Wang, K., Fan, Q. and Li, H.L. (2015) Optimization and Application of Monitoring Location of Deep Foundation Pit. *Mine Survey*, **4**, 50-52+55.

[27] Tao, X.P., Yuan, J.X., Zhang, Y., *et al.* (2022) Displacement Monitoring and Deformation Analysis of Foundation Pit. *Tianjin Construction Science and Technology*, **32**, 39-43.

[28] Xue, X.L., Zeng, C.F. and Zheng, G. (2019) Deformation Characteristics and Control Methods of Foundation Pit Induced by Dewatering before Excavation. *Chinese Journal of Underground Space and Engineering*, **15**, 492-497.

[29] Wu, X., Feng, Z., Liu, J., Chen, H. and Liu, Y. (2024) Predicting Existing Tunnel Deformation from Adjacent Foundation Pit Construction Using Hybrid Machine Learning. *Automation in Construction*, **165**, Article 105516. https://doi.org/10.1016/j.autcon.2024.105516

[30] Miao, X. and Zhao, H. (2024) Maximum Pitting Corrosion Depth Prediction of Buried Pipeline Based on Theory-Guided Machine Learning. *International Journal of Pressure Vessels and Piping*, **210**, Article 105259. https://doi.org/10.1016/j.ijpvp.2024.105259

[31] Wang, H.C., Li, S., Lin, L., *et al.* (2021) Prediction of Adjacent Tunnel Deformation Caused by Foundation Pit Excavation Based on BP Model. *Chinese Journal of Underground Space and Engineering*, **17**, 832-839+847.

[32] Xu, C.J. and Li, X.Y. (2024) Lateral Deformation Prediction of Deep Foundation Retaining Structures Based on Artificial Neural Network. *Journal of Shanghai Jiaotong University*, **58**, 1-20.

[33] Ni, X.D., Zhang, Y.K., Yan, L., *et al.* (2024) Prediction of Super Large Deformation of Deep Foundation Pit Based on HSS-MCC Fusion Model and SSA-BP Neural Network. *Journal of Hunan University* (*Natural Sciences*), **51**, 35-45.